Polymer 49 (2008) 2342–2353

Contents lists available at ScienceDirect

Polymer

journal homepage: www.elsevier.com/locate/polymer

A morphological study of poly(butylene succinate)/poly(butylene adipate) blends with different blend ratios and crystallization processes

Haijun Wang [a], Zhihua Gan [a,*], Jerold M. Schultz [b], Shouke Yan [a,*]

[a] Joint Laboratory of Polymer Sciences and Materials, Institute of Chemistry, The Chinese Academy of Sciences, Beijing 100080, China
[b] Department of Chemical Engineering, University of Delaware, Newark, DE 19716, USA

ARTICLE INFO

Article history:
Received 18 January 2008
Received in revised form 11 February 2008
Accepted 26 February 2008
Available online 7 March 2008

Keywords:
Poly(butylene succinate)
Poly(butylene adipate)
Blends

ABSTRACT

Morphologies of PBS/PBA blends varying in blend ratio at different crystallization temperatures of PBS component were studied using optical and atomic force microscopies. It was found that interspherulitic phase segregation of PBA takes place at high temperature, e.g. 100 °C, for all blend compositions due to the high diffusion length. On the contrary, no interspherulitic phase segregation of PBA at 75 °C occurs at all, consistent with a shorter diffusion length. It was further found that the PBA melt acted as a diluter, affecting the morphology of PBS, which in turn influenced the phase separation behavior of PBA remarkably. At 100 °C, with increasing PBA concentration, the resultant open structure of PBS caused by the diluting effect of the PBA melt makes it necessary to retain some portion of the PBA melt between the PBS lamellae. This leads to the concurrence of interlamellar and interspherulitic phase segregations. An even higher PBA content results in the occurrences of all three phase separation options, i.e. interlamellar, interfibrillar and interspherulitic phase segregations. At 75 °C, in blends with PBA as a minority phase, mainly interlamellar segregation of PBA occurs. For a 50/50 blend, interlamellar and interfibrillar phase segregations take place simultaneously. For a PBA in-rich blend, PBS forms only a spherulitic framework, filled in with the PBA lamellar crystals, indicating that interfibrillar mode is the main phase separation process.

1. Introduction

Blending one polymeric material with another is of scientific and industrial interest as a means for developing new polymeric materials with desirable property combinations without having to synthesize novel polymers. Binary polymer systems may be of amorphous/amorphous, crystalline/amorphous, and crystalline/crystalline blend types. It has become of interest to study polymer blends containing at least one component capable of crystallizing, since a certain degree of crystallinity is normally important in order to ensure satisfactory high-temperature strength and environmental resistance. In these systems, liquid–solid phase separation during the crystallization of one component can lead to a large variety of morphologies [1–7]. Especially in crystalline/crystalline polymer blends, the difference in the melting points of the two components can lead to the systems existing in amorphous/amorphous, crystalline/amorphous and crystalline/crystalline states depend upon the temperature. As a result, much more complicated crystalline morphologies can be created in crystalline/crystalline polymer blends, compared with the crystalline/amorphous polymer blends.

Till now, many crystalline/crystalline polymer blend systems have been studied [8–16]. For these studies, the morphological developments of the polymer blend systems have most frequently been studied by optical microscopy, scattering and diffraction, and spectroscopies. There are only few reports of microscopic observations at the lamellar scale [17–19]. Therefore, we present here a detailed morphological observation of poly(butylene succinate)/poly(butylene adipate) (PBS/PBA) blends using optical and atomic force microscopies.

The purpose of this paper is to probe the effects of temperature and composition on the morphologies of these blends. On the basis of the observed morphologies, the phase separation of PBA during the crystallization process of PBS is discussed. The results given here largely confirm the morphological detail that less direct methods have suggested. The results also demonstrate the role of diffusion ahead of the growth front.

2. Experimental

2.1. Materials

The PBA material used in this work was produced by BASF AG and has a weight-average molecular weight of about 3.5×10^4 g/mol,

* Corresponding authors. Tel./fax: +86 10 82618476.
E-mail addresses: zhgan@iccas.ac.cn (Z. Gan), skyan@iccas.ac.cn (S. Yan).

0032-3861/$ – see front matter © 2008 Elsevier Ltd. All rights reserved.
doi:10.1016/j.polymer.2008.02.050

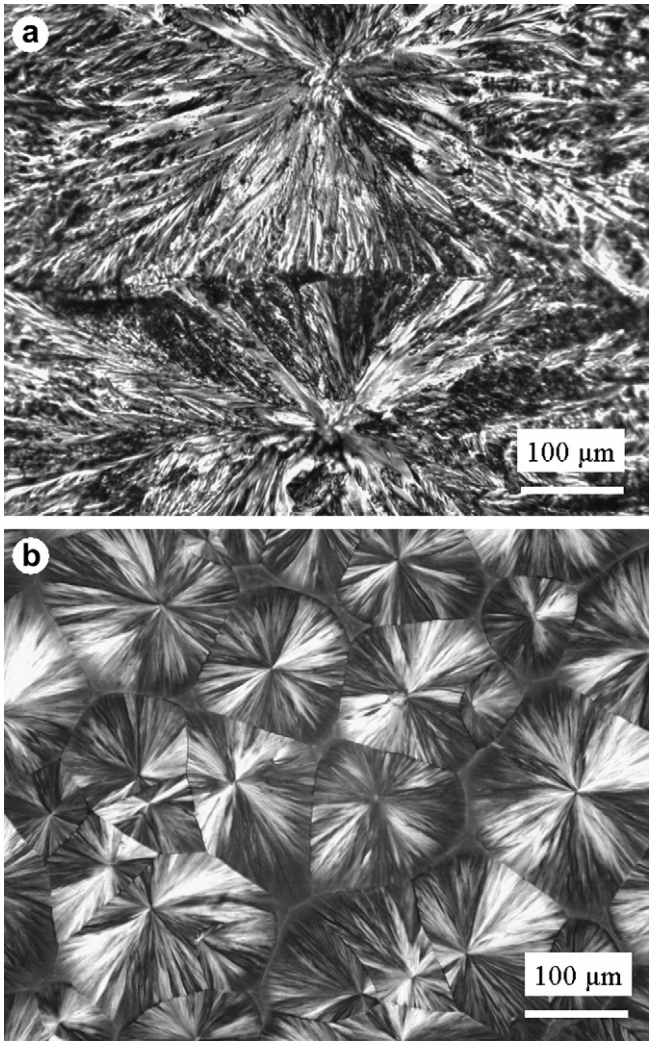

Fig. 1. Optical micrographs of the spherulitic morphology of neat PBS crystallized at (a) 100 °C and (b) 75 °C.

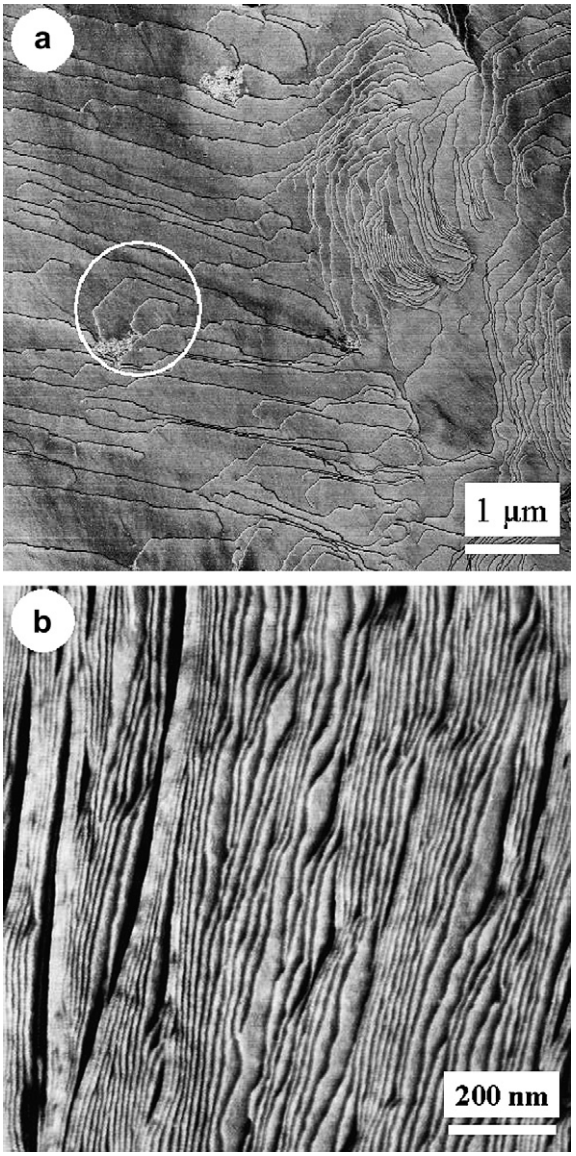

Fig. 2. Lamellar morphologies of neat PBS using AFM phase contrast: (a) crystallized isothermally at 100 °C and (b) crystallized isothermally at 75 °C. Scanned at 25 °C.

with a polydispersity of 1.7. PBS with an M_w of 200,000 g/mol was purchased from Aldrich Chemical. The melting points of PBS and PBA are measured to be 114 °C and 60 °C, respectively. Both materials have been purified again by precipitating from their chloroform solutions before use.

2.2. Preparation

Blends of PBS and PBA were prepared by solution blending with chloroform as a common solvent. Both were dissolved in chloroform with desired mass proportions (total polymer concentration was 30 mg/mL). Thin films for optical microscopy (OM) and atomic force microscopy (AFM) observations were prepared by casting the solution on clean glass slides. The thickness of the resultant films was estimated to be about 100 μm. After evaporation of the solvent, thin films both for AFM and OM observations have been subjected to the following thermal treatment. The samples were heated to and kept at 140 °C for 15 min to eliminate previous thermal history completely, then cooled to the preset isothermal crystallization temperatures of PBS: either 3 h at 75 °C or 2 weeks at 100 °C. From either of these temperatures, the specimen was finally cooled to the crystallization temperatures of the PBA component. The crystallization temperature of PBA was set either at 30 °C or at 0 °C, which is indicated in detail in each of the figure captions, for a good visualization of the PBA phase.

2.3. Characterizations

An Olympus BH-2 microscope equipped with a Linkam LK-600PM temperature controller was used in this study. All of the optical micrographs shown in this paper were taken under crossed polarizers. Tapping-mode AFM images were obtained using a NanoScope III MultiMode AFM (Digital Instruments) equipped with a high-temperature heater accessory (Digital Instruments). Si cantilever tips (TESP) with a resonance frequency of approximately 300 kHz and a spring constant of about 40 Nm^{-1} were used. The scan rate varied from 0.7 to 1.2 Hz. The scanning density was 512 lines/frame. The set-point amplitude ratio, A_{sp}/A_o, was adjusted to 0.7–0.9, where A_{sp} is the set-point amplitude and A_o is the amplitude of the free oscillation. The phase contrast imaging

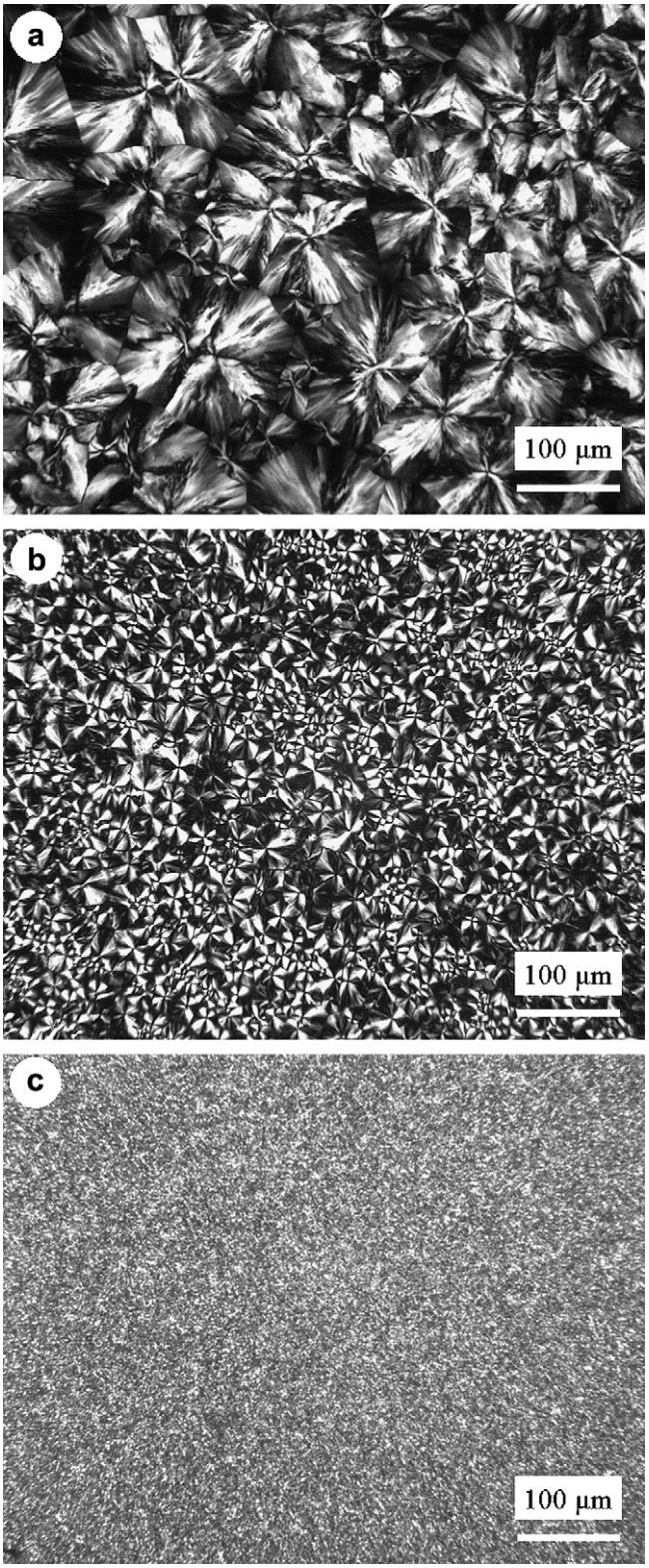

Fig. 3. Optical micrographs of the spherulitic morphology of neat PBA crystallized at (a) 50 °C; (b) 30 °C, and (c) 0 °C.

technique was utilized to distinguish between the amorphous and crystalline phases. The AFM images were obtained either at 25 °C to show the overall structure or at 70 °C to melt away the PBA crystals.

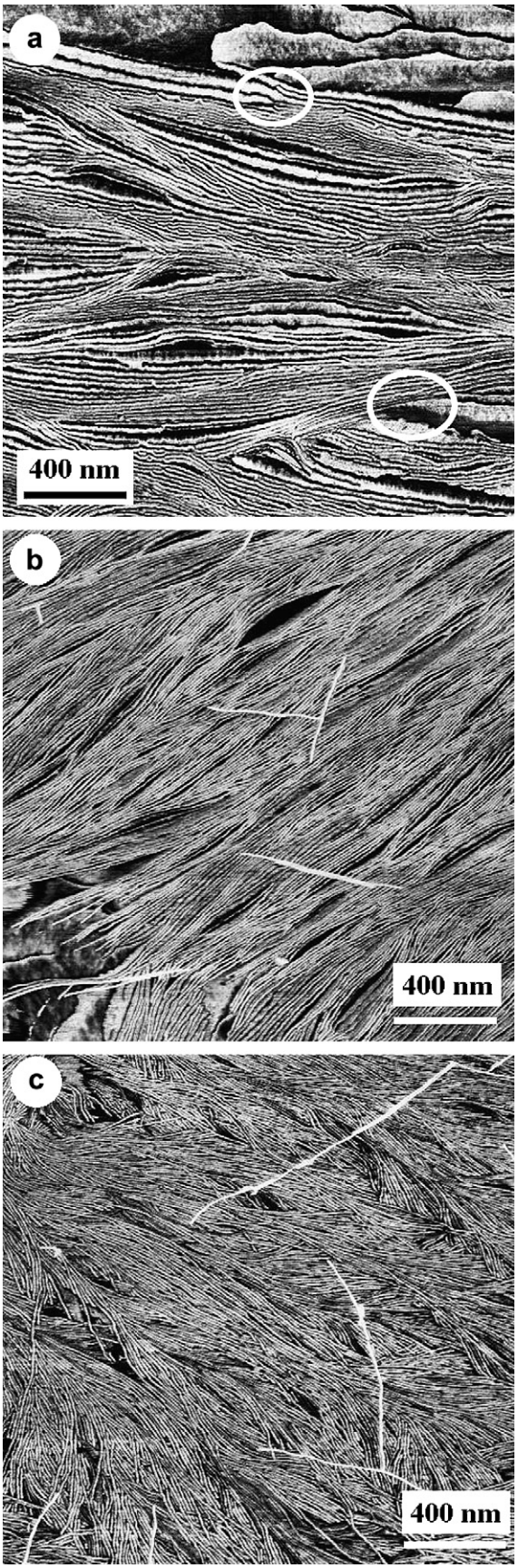

Fig. 4. AFM phase images of neat PBA crystallized isothermally at (a) 50 °C; (b) 30 °C, and (c) 0 °C. Scanned at 25 °C.

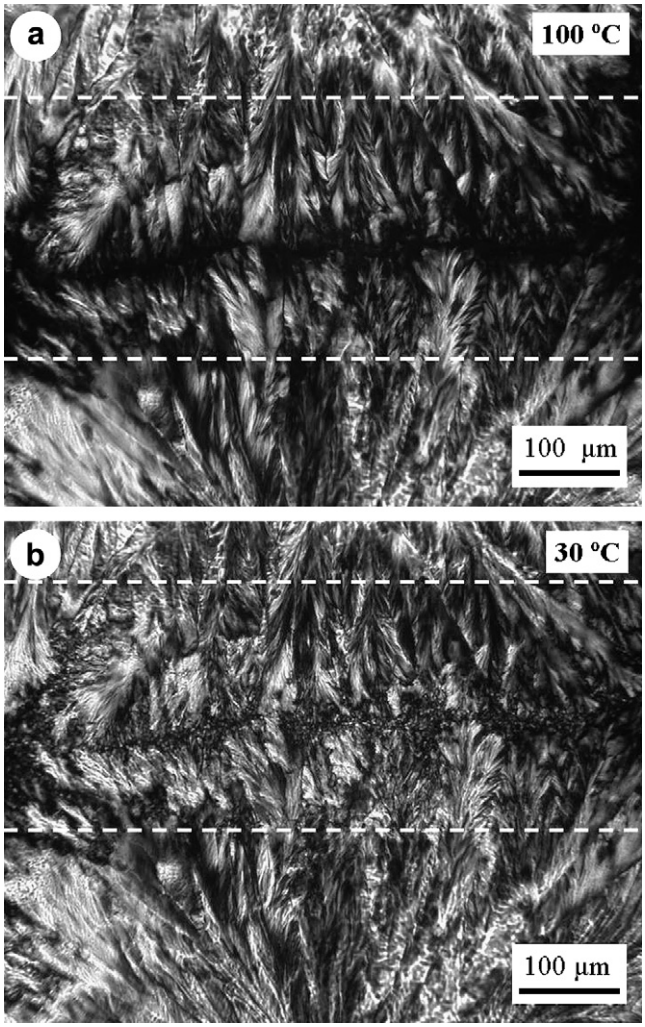

Fig. 5. Optical micrographs of an 80/20 PBS/PBA blend under two-step crystallization conditions. (a) PBS crystallized isothermally at 100 °C for 2 weeks, and (b) after crystallization of PBA at 30 °C for 2 h.

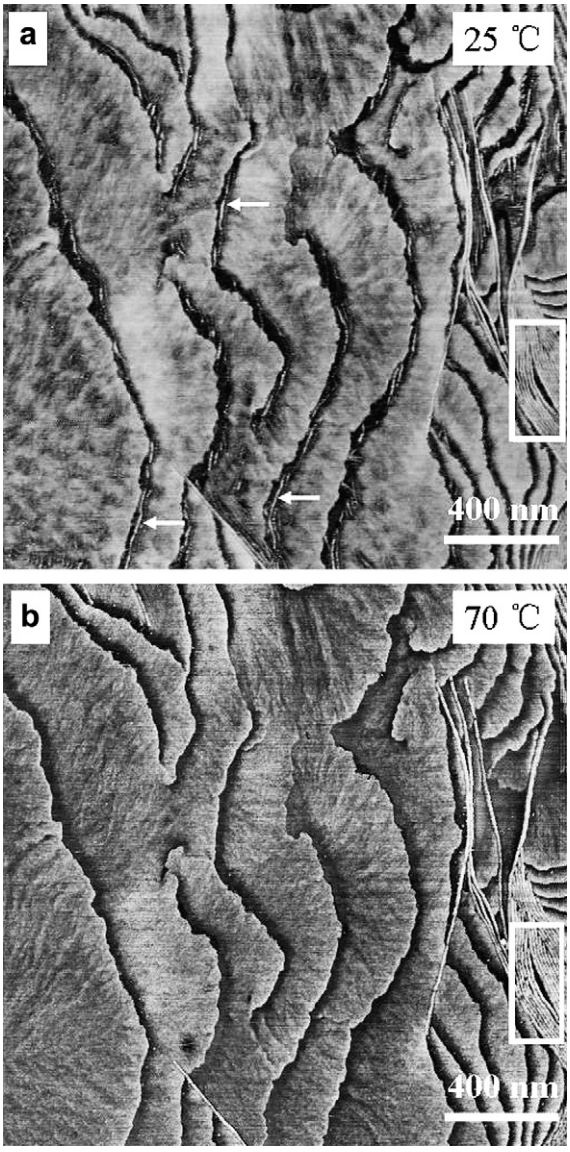

Fig. 6. AFM phase images of an 80/20 PBS/PBA blend with PBS crystallized isothermally at 100 °C for 2 weeks before cooling to 0 °C. The images were scanned (a) at 25 °C and (b) at 70 °C.

3. Results

3.1. Morphologies of neat PBS and PBA

For a better understanding of the morphological details of the PBS/PBA blend systems, the morphologies of neat PBS and PBA were first examined by optical and atomic force microscopies. Fig. 1a and b show the optical micrographs of PBS crystallized at 100 °C and 75 °C, respectively. The morphological features of the PBS spherulites are rather different, depending on the crystallization temperatures. On crystallization at 100 °C (Fig. 1a), PBS spherulites grow in hundreds of microns. These large spherulites possess open and irregular structures. The boundaries between these spherulites are consequently somewhat hazy. With decreasing crystallization temperature (Fig. 1b) smaller spherulites with compact (close and regular) structure of about 100 μm in diameter are observed. The decrease in spherulite size is caused by the increment in nucleus number originating from high nucleation density under large supercooling. The different structure features of the PBS spherulites generated at different temperatures can be more clearly visualized by fine intraspherulitic structure characterization.

Fig. 2 shows the corresponding AFM phase images of the PBS spherulites shown in Fig. 1. Lamelli-form crystals seen face-on are the predominant structures in the PBS spherulite grown at 100 °C (Fig. 2a). With careful inspection, it is found that some of the lamellar crystals exhibit well-defined regular facets (see the circled region in Fig. 2a). For isothermal crystallization at 75 °C, as shown in Fig. 2b, PBS forms mainly lamellae seen on edge. The edge-on lamellae align parallel for a long distance. Some of these crystalline lamellae rotate into a flat-on orientation. This result is quantitatively consistent with Kanamoto's results [20].

Fig. 3 shows optical micrographs of PBA thin films isothermally crystallized at different temperatures. The PBA spherulites become increasingly smaller with decreasing crystallization temperature. When crystallizing PBA at 50 °C, spherulites of approximately 100 μm in diameter can be observed; at 30 °C the size is about 50 μm. At even lower temperature, e.g. 0 °C, the spherulitic structure is barely recognizable under optical microscopy. AFM observation revealed that PBA grows dominantly in edge-on lamellar form in the temperature range of 30–50 °C, as seen in Fig. 4a and b. Some small domains are occasionally observed with lamellae viewed flat-on (top and right bottom corner of Fig. 4a). The flat-on

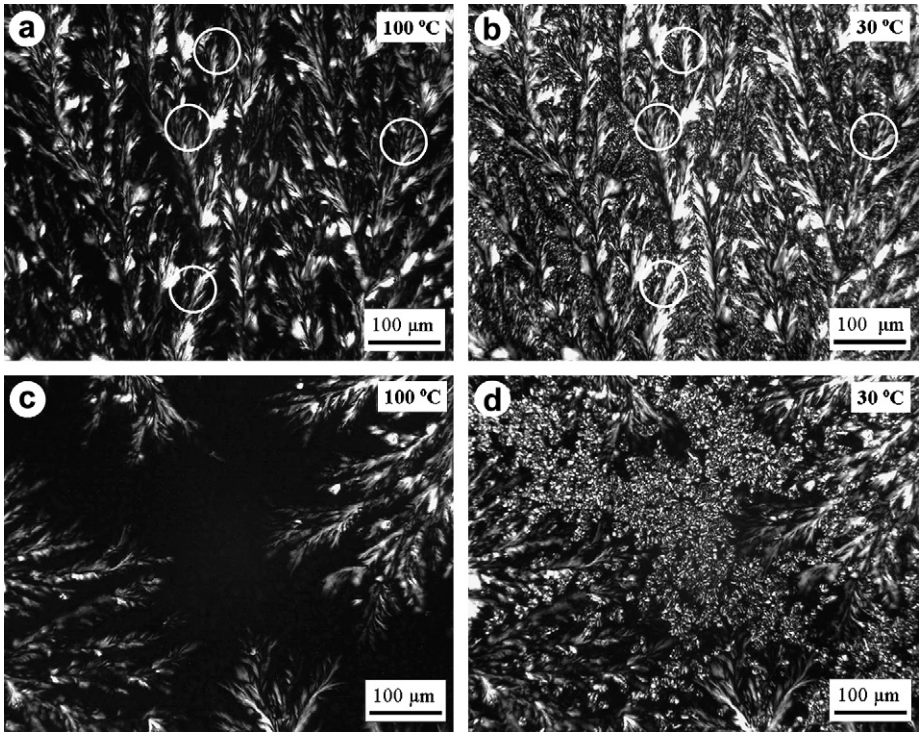

Fig. 7. Optical micrographs illustrate the morphologies of a 50/50 PBS/PBA blend crystallized first at 100 °C for 2 weeks (a and c), and then at 30 °C for 2 h (b and d).

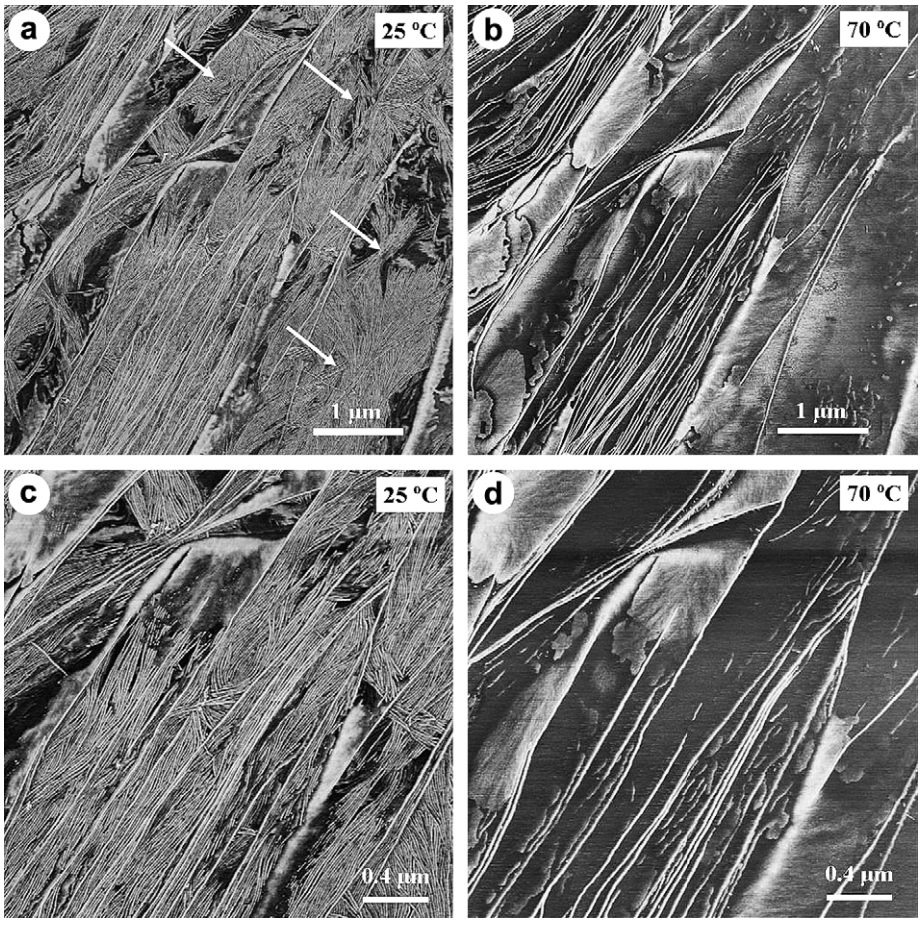

Fig. 8. AFM phase images of a 50/50 PBS/PBA blend with PBS crystallized at 100 °C for 2 weeks and then cooled at a rate of 30 °C/min to 0 °C. The images were scanned at 25 °C (a and c) and 70 °C (b and d), respectively.

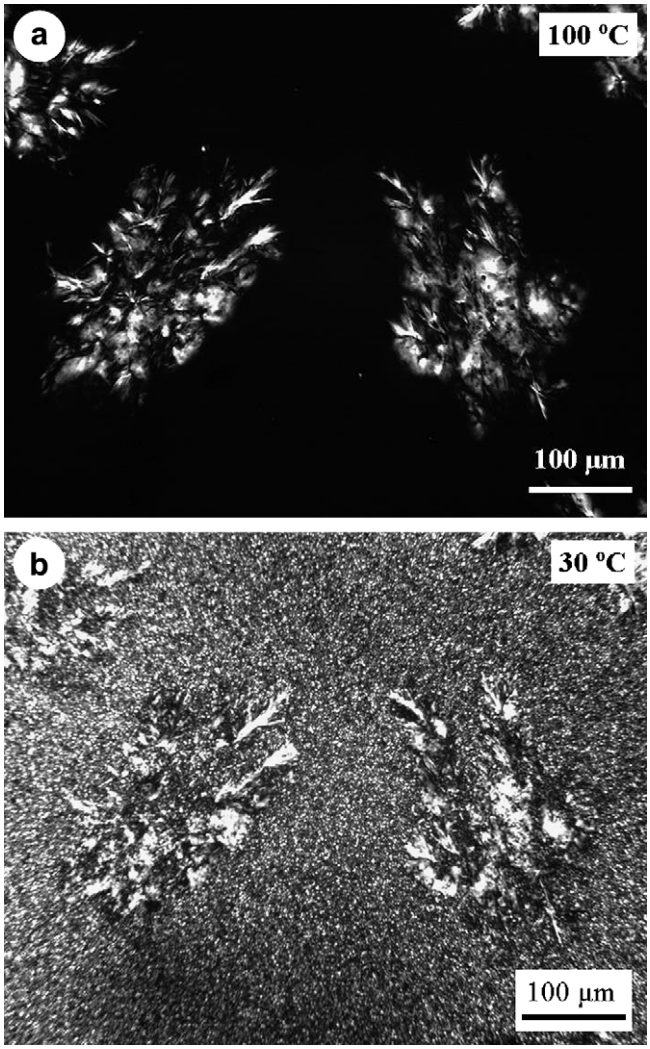

Fig. 9. Optical micrographs of a 20/80 PBS/PBA blend, which was crystallized at (a) 100 °C for 2 weeks and (b) 30 °C for 2 h.

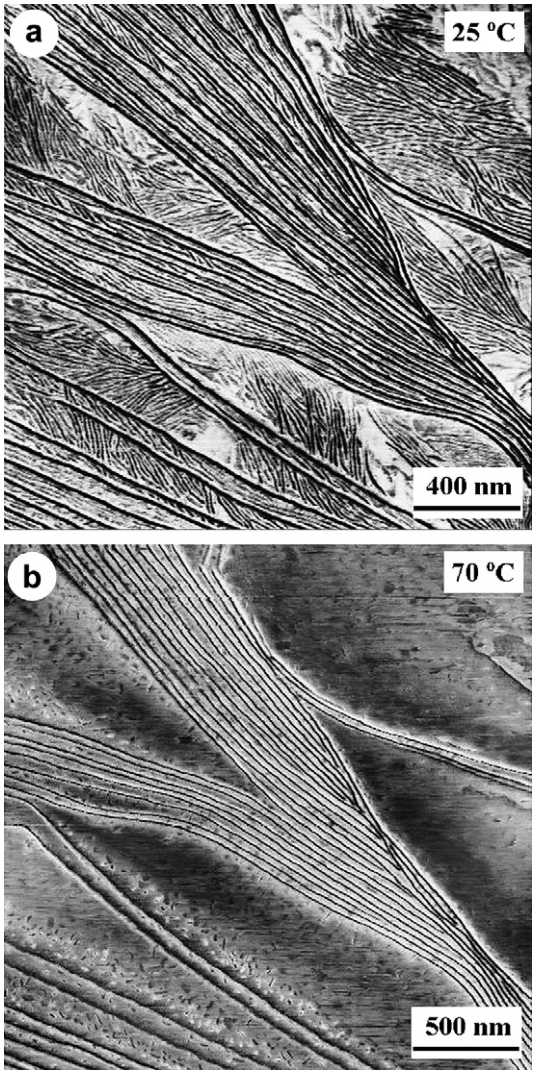

Fig. 10. AFM phase images of a 20/80 PBS/PBA blend, which was first crystallized at 100 °C for 2 weeks and then cooled at a rate of 30 °C/min to 0 °C. The images were scanned at (a) 25 °C and (b) 70 °C.

lamellae originated from the twisting of their edge-on counterparts, as can be judged from the part circled in Fig. 4a. These domains become smaller and less frequent with decreasing crystallization temperature. When quenching the PBA melt direct into ice water at 0 °C (Fig. 4c), only edge-on lamellae are observed in the whole sample.

3.2. Morphologies of PBS/PBA blends with PBS crystallized at 100 °C

Fig. 5 shows representative optical micrographs of an 80/20 PBS/PBA blend taken during the crystallization process. Keeping the sample at 100 °C for 2 weeks (Fig. 5a), crystallization of PBS takes place, while PBA remains molten. In Fig. 5a, one sees two spherulites, one growing down from above and the other growing upward from below the field of view. The birefringence in the optical micrograph comes from the PBS crystals solely. It should be mentioned that the spherulites in this 80/20 blend are larger than those for the neat PBS, indicating a reduction of nucleation density (probably caused by the diluting effect of PBA). When the sample was cooled to 30 °C, PBA crystallized, which resulted in an increment of the birefringence of the sample. With careful comparison of Fig. 5a with Fig. 5b, we find that the enhancement of the birefringence occurs mainly in the boundary area of the PBS spherulites, i.e. between the two dashed lines. This observation demonstrates that the PBA component in the PBS/PBA (80/20) system crystallized isothermally first at 100 °C and then 30 °C locates mainly in the interspherulitic regions of the PBS spherulites.

To determine whether there is some PBA dispersed in the inner part of the PBS spherulite, the fine structure of the blend is monitored using AFM with a hot stage. The sample used for AFM observation is in principle the same as that used for optical microscopy experiment except for the change of crystallization temperature for the PBA component. Instead of 30 °C used for optical microscopy study, 0 °C was used for AFM experiment in order to simplify the differentiation of the PBA and PBS crystals. A representative AFM phase image taken at the inner part of a PBS spherulite crystallized first at 100 °C for 2 weeks and then quenched into ice water is shown in Fig. 6a. As in the case of pure PBS crystallized at 100 °C (Fig. 2a), the sample exhibits mainly flat-on crystals. Considering that the PBA crystallizes at 0 °C in fully edge-on lamellar crystals, the observed morphology implies that the inner part of the spherulite in this 80/20 PBS/PBA blend is indeed mainly composed of PBS. There are small regions, as indicated by a rectangle at the right margin of Fig. 6a, with some lamellae seen on edge. Also, some short lamellar crystals dispersed sporadically at the growth fronts of the flat-on PBS

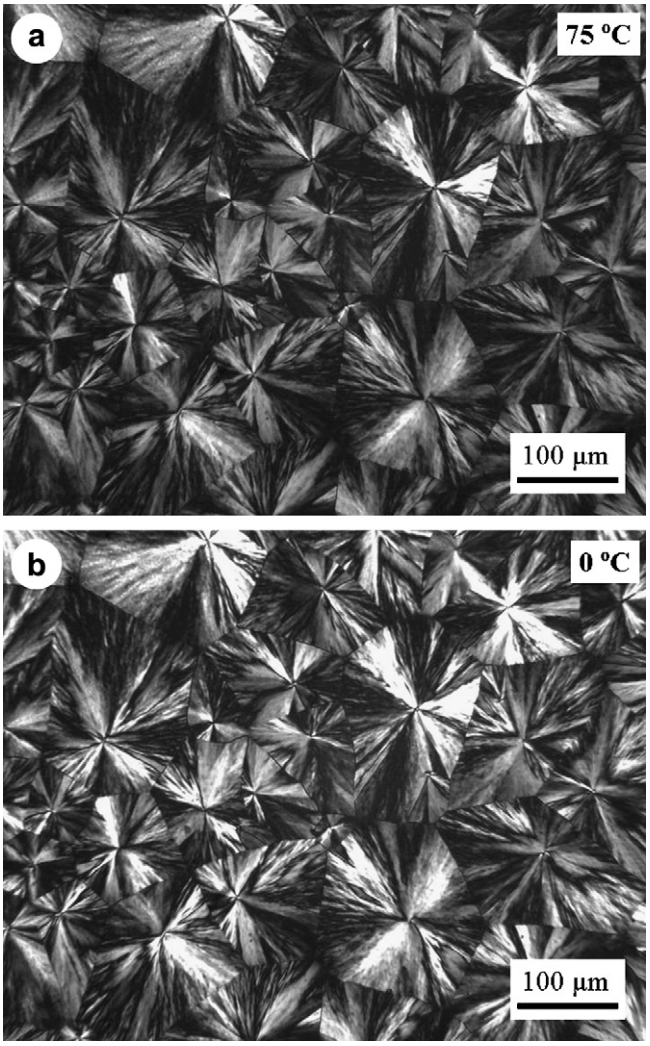

Fig. 11. Optical micrographs of an 80/20 PBS/PBA blend prepared by a two-step crystallization conditions: (a) crystallization of PBS at 75 °C for 2 h and (b) crystallization of PBA at 0 °C.

crystals can be observed. Three of these are marked by white arrows. To find out whether these lamellar crystals pertain to PBA or not, selective melting of the sample was performed in situ during the AFM experiment. As illustrated in Fig. 6b, after heating the sample to 70 °C (well above the melting temperature of PBA, but below the melting of PBS), the short lamellae at the growth fronts of the PBS crystals disappeared, while those in the rectangular part remained. This clearly indicates that only the short edge-on lamellae at the growth fronts of PBS are PBA crystals. These results confirm that PBA in an 80/20 blend prepared at present crystallization condition locates mainly in the boundary and the interspherulitic regions of the PBS spherulites.

Increasing the content of PBA changes the morphology of PBS. Nevertheless, PBS always exhibits a spherulitic structure. Fig. 7 shows polarized optical micrographs of two areas of a 50/50 PBS/PBA blend crystallized first isothermally at 100 °C for 2 weeks and then at 30 °C for 2 h. The areas of Fig. 7a and b are interior to a PBS spherulite, whereas Fig. 7c and d are at the intersection of three spherulites. The PBS spherulites have become more open, especially in the margin areas of the spherulites. As shown in Fig. 7c, a large domain of hundreds of microns remains non-birefringent between the PBS spherulites. This indicates that there exist no crystals in this area at 100 °C. During the cooling, no birefringent changes have been recognized in both parts a and c of Fig. 7 at temperatures above the melting point of PBA, indicating the completion of crystallization of PBS at 100 °C for 2 weeks. Therefore, the morphological change during further cooling process is mainly caused by crystallization of the PBA component. As illustrated in parts b and d of Fig. 7, the birefringence of the sample changed markedly when the sample was cooled to 30 °C for 2 h, reflecting the crystallization of PBA. One may notice that the initially both dark interfibrillar and interspherulitic areas exhibit birefringence. This indicates that most of the PBA component in the PBS/PBA (50/50) system crystallized isothermally first at 100 °C and then 30 °C locates in the interspherulitic regions of the PBS spherulites. With careful inspection, an intensity increment of some microdomains already showing birefringence before crystallization of PBA can be identified; compare the circled parts in Fig. 7a and b. This implies the existence of some PBA in this 50/50 PBS/PBA blend crystallizing in the interlamellar regions of the PBS spherulite.

AFM observation confirms the above optical microscopy result. Fig. 8 shows AFM phase images of a 50/50 PBS/PBA blend with PBS crystallized at 100 °C and PBA crystallized at 0 °C. Fig. 8a and c was scanned at 25 °C, while Fig. 8b and d were scanned at 70 °C, at which the PBA crystals are molten. It was found that the morphology in the interspherulitic area has a close resemblance to that of neat PBA (figure not shown), reflecting the existence of the PBA materials between the PBS spherulites. In the inner part of the PBS spherulite, as shown in Fig. 8a, one can find individual PBA spherulites (indicated by white arrows), which contribute to the appearance of the birefringence in the initial dark interfibrillar parts. Selective melting of the PBA crystals at 70 °C (Fig. 8b) helps us to locate where PBA has been; the image reflects only the PBS crystals. Comparing Fig. 8b with Fig. 8a, one can also find that some PBA crystalline lamellae have melted from the interlamellar regions of PBS. This is more clearly seen in the enlarged micrograph shown in parts c and d of Fig. 8. The AFM results demonstrate that there is indeed some PBA crystallizing in the interlamellar regions of the PBS spherulite, while most of it crystallizes in the interfibrillar and interspherulitic areas.

It should be pointed out that the morphology of PBS itself changes considerably with increasing PBA content; compare Fig. 8b and d with Figs. 2a and 6a. In addition to forming more skeletal (dendritic) spherulites, now a large portion of PBS grows in edge-on lamellar crystals, while some small domains still exhibit flat-on orientation.

With further increase in the PBA content to 80%, PBS still forms spherulitic structures during isothermal crystallization at high temperature. The PBS spherulites, however, can no longer fill in the entire. As an example, Fig. 9a shows an optical micrograph of a 20/80 PBS/PBA blend crystallized isothermally at 100 °C for 2 weeks. There exist a few PBS spherulites well separated from each other. After crystallizing the PBA component at 30 °C (Fig. 9b), a profusion of PBA microcrystallites fill the interspherulitic regions. There are also some PBA crystals dispersed within the PBS spherulitic regions, as judged from the birefringence change within the PBS spherulites. This is more clearly revealed by AFM observation. As seen in Fig. 10a, now both PBS and PBA crystallize in edge-on lamellar form, with the long, thicker PBS lamellae forming a scaffold which is filled in by the short, thinner PBA lamellae. The thin PBA lamellae grow either between the PBS crystalline lamellae or between PBS lamellar stacks. Comparing Fig. 10a with the partially molten one shown in Fig. 10b, one can more clearly identify the above-described structure.

3.3. Morphologies of PBS/PBA blends with PBS crystallized at 75 °C

Fig. 11a shows a representative polarized light micrograph of an 80/20 PBS/PBA blend after heat treatment at 140 °C for 15 min and

then cooled to 75 °C. It is clear that the PBS crystallizes now in compact spherulites after the completion of its crystallization at 75 °C for 2 h. The PBS spherulites cover the whole area. The existence of a well-defined spherulite boundary indicates that no PBA melt is expelled into the interspherulitic regions. This is different from the case of PBS crystallized isothermally at 100 °C (Fig. 5). Fig. 11b illustrates the morphological change after cooling the blend from 75 °C to 0 °C. We can recognize an overall intensity increase in birefringence of the PBS spherulites. This again demonstrates that the crystallization of PBA takes place within the PBS spherulitic regions. To find out the exact location of the PBA crystals, the fine structure of the blend after completion of crystallization for both components was examined using AFM. Fig. 12a shows a representative AFM phase image of the above used sample. Fig. 12c is a higher resolution image of a portion of Fig. 12a. Here we see mainly edge-on lamellae in the radial direction of the PBS spherulite. Although in some places, as indicated by the white arrows, the PBA edge-on lamellae can be distinguished from the PBS ones by careful inspection, selective melting of the PBA lamellae is still necessary for identifying the PBS lamellae more clearly. Fig. 12b shows the same sample area as Fig. 12a scanned at 70 °C. Disappearance of the PBA lamellae at this temperature makes it clear that the some of the PBA component crystallizes as thinner lamellae (with respect to the PBS ones) inserted in the PBS interlamellar regions, while the rest accumulates between the lamellar bundles (fibrils) of PBS and forms microdomains of stacked edge-on lamellae. This is more clearly seen in the magnified AFM phase images (Fig. 12c and d).

For a 50/50 PBS/PBA blend, during isothermal crystallization at 75 °C, PBS forms still larger spherulites with fairly straight impinging edges (the pictures are similar to those shown in Fig. 11, and therefore not shown here again), indicating that no PBA melt accumulates in the boundary areas of the PBS spherulites. The more open structure of the PBS spherulites compared with that formed in pure PBS and its 80% blend implies that the increase of PBA component within the spherulites results in an even sparser arrangement of the PBS crystals. A uniform intensity increment of the birefringence of the PBS spherulites after crystallization of PBA at 0 °C helps us to conclude that the PBA component is evenly dispersed in the PBS spherulites. AFM observation confirms that the PBA lamellae are partly inserted between the PBS lamellae and partly segregated between the PBS lamellar bundles with a larger domain size than that in the 80/20 PBS/PBA blend.

In a PBA-rich blend, e.g. 20/80, through isothermal crystallization at 75 °C, PBS forms still sparsely arranged spherulites. As shown in Fig. 13a, the PBS spherulites have covered the whole area of the sample, with the PBS crystals revealed as uniformly dispersed birefringent spots in the optical micrograph. This is quite different from the case of crystallizing PBS at 100 °C isothermally; compare Fig. 13a with Fig. 9a. The open spherulitic structure makes it difficult to identify the impinging edges of the spherulites. Nevertheless, an even dispersion of the PBA melt in the blend can be judged according to the optical micrograph shown in Fig. 13a. The morphological change of the blend after the subsequent crystallization of PBA at 0 °C, Fig. 13b, also supports this conclusion. Fig. 14a and b presents the AFM phase images of a 20/80 blend used in

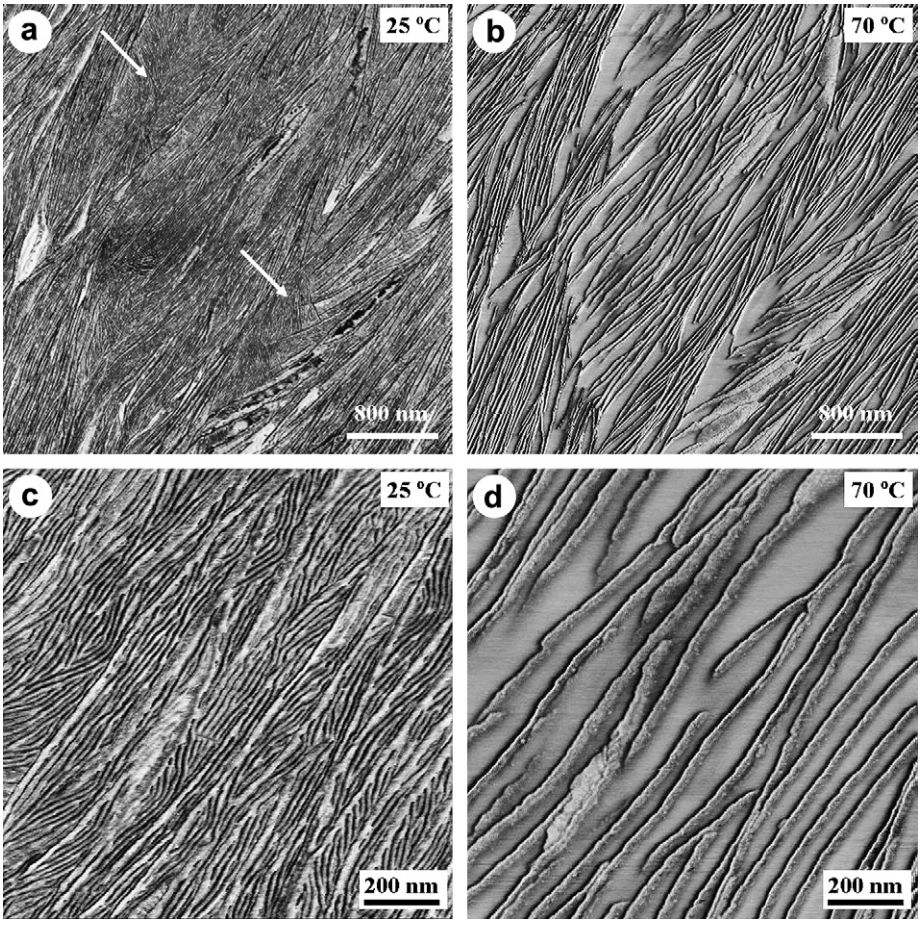

Fig. 12. AFM phase images of an 80/20 PBS/PBA blend with PBS crystallized at 75 °C for 2 h and then cooled at a rate of 30 °C/min to 0 °C. The images were scanned at 25 °C (a and c) and 70 °C (b and d).

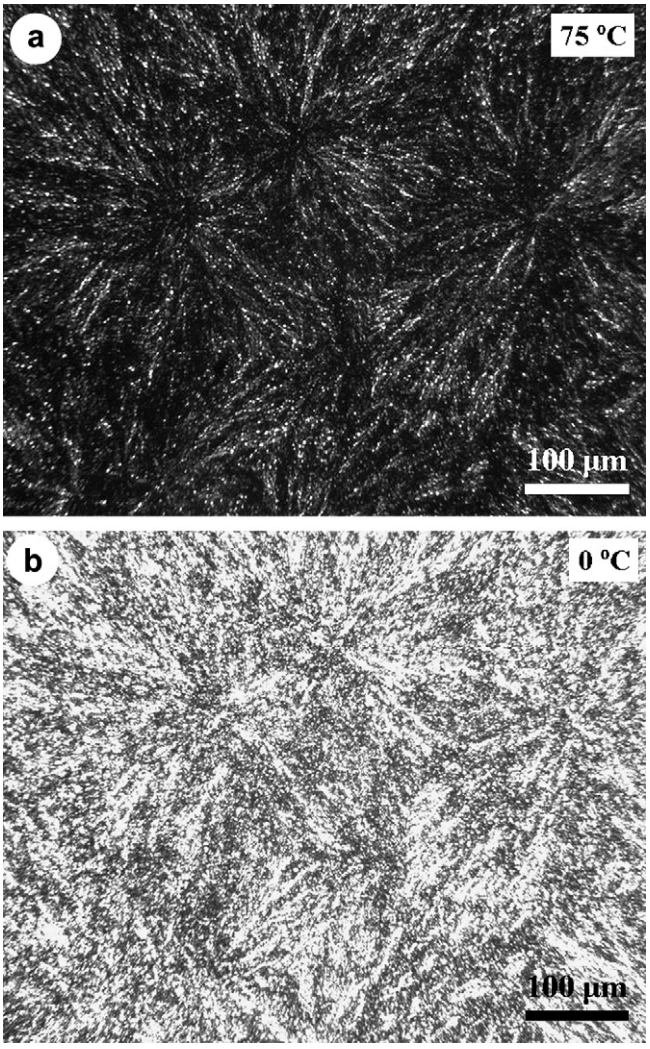

Fig. 13. Optical micrographs of a 20/80 PBS/PBA blend prepared by a two-step crystallization conditions: (a) crystallization of PBS at 75 °C for 2 h and (b) crystallization of PBA at 0 °C.

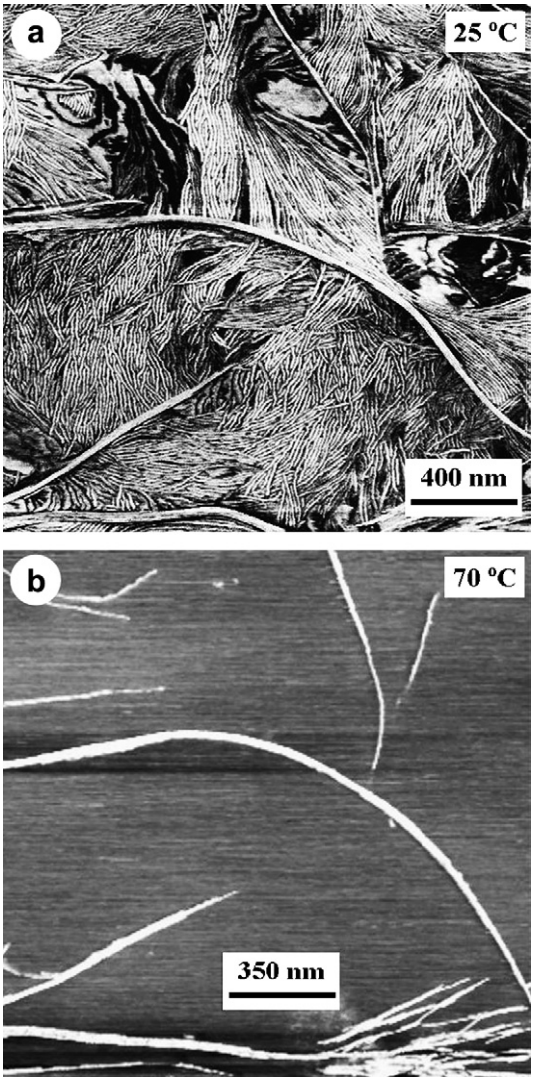

Fig. 14. AFM phase images of a 20/80 PBS/PBA blend with PBS crystallized at 75 °C for 2 h and then cooled at a rate of 30 °C/min to 0 °C. The images were scanned at (a) 25 °C and (b) 70 °C.

Fig. 13 scanned at 25 °C and 70 °C, respectively. From Fig. 14, it can be seen that, in the 20/80 PBS/PBA blend, the PBS crystalline lamellae construct only a scaffold framework, while the PBA lamellae crystals grow in the PBS scaffold and fill in the whole space. The domains of the aggregated PBA lamellar crystals are now of micrometer size.

4. Discussion

The sketches in Fig. 15 serve to illustrate the significant points of the above observations. During the crystallization of PBS in a PBS/PBA blend at 100 °C, when the PBA content is low, e.g. 20%, it mainly accumulates in the interspherulitic regions of PBS (Fig. 15a). With increasing amount of PBA in the blend, some of PBA have been embedded into the interlamellar and interfibrillar regions of PBS, while most of PBA locates still in the interspherulitic regions of PBS, see Fig. 15b. For a PBA-rich blend, as sketched in Fig. 15c, while most of the PBA crystals fill in the remaining open areas, some of the PBA crystalline lamellae are dispersed in the interlamellar as well as the interfibrillar regions of PBS. During the crystallization of PBS at 75 °C, PBS forms spherulites covering the whole area, regardless of its concentration in the blends. Therefore, the PBA melt is dispersed in the intraspherulitic regions of PBS at all blend ratios. At low PBA ratio, e.g. 20%, PBA is mainly dispersed in the interlamellar regions of PBS (Fig. 15d). With increasing amount of PBA in the blend (50%), except for the part of PBA inlaid into the interlamellar regions of PBS, most of PBA aggregates to form small homogeneous domains with edge-on lamellar orientation (Fig. 15e). In a PBA in-rich blend, e.g. a 20/80 PBS/PBA blend, PBS forms only a spherulitic scaffold covering the whole area, while the PBA crystals fill in the scaffold, forming domains with aggregates of edge-on lamellae (Fig. 15f).

The observed structures can be produced in the following ways: (i) phase separation takes place before crystallization and crystallization of both components successively in phase separated blend system causes the observed structure; (ii) PBA is expelled out during the crystallization of the PBS component; or even (iii) a combination of the (i) and (ii). Considering that PBA $(-O-(CH_2)_4-O-CO-(CH_2)_4-CO-)_n$ and PBS $(-O-(CH_2)_4-O-CO-(CH_2)_2-CO-)_n$, are chemically very similar, full miscibility in the melt would be expected and blends in this system should exhibit no liquid/liquid phase separation. This was confirmed by glass transition temperature (T_g) measurement since only single T_g was detected for each blend with its value decreased from −41.8 °C (pure PBS) to −60.3 °C (pure PBA). To further confirm that the observed

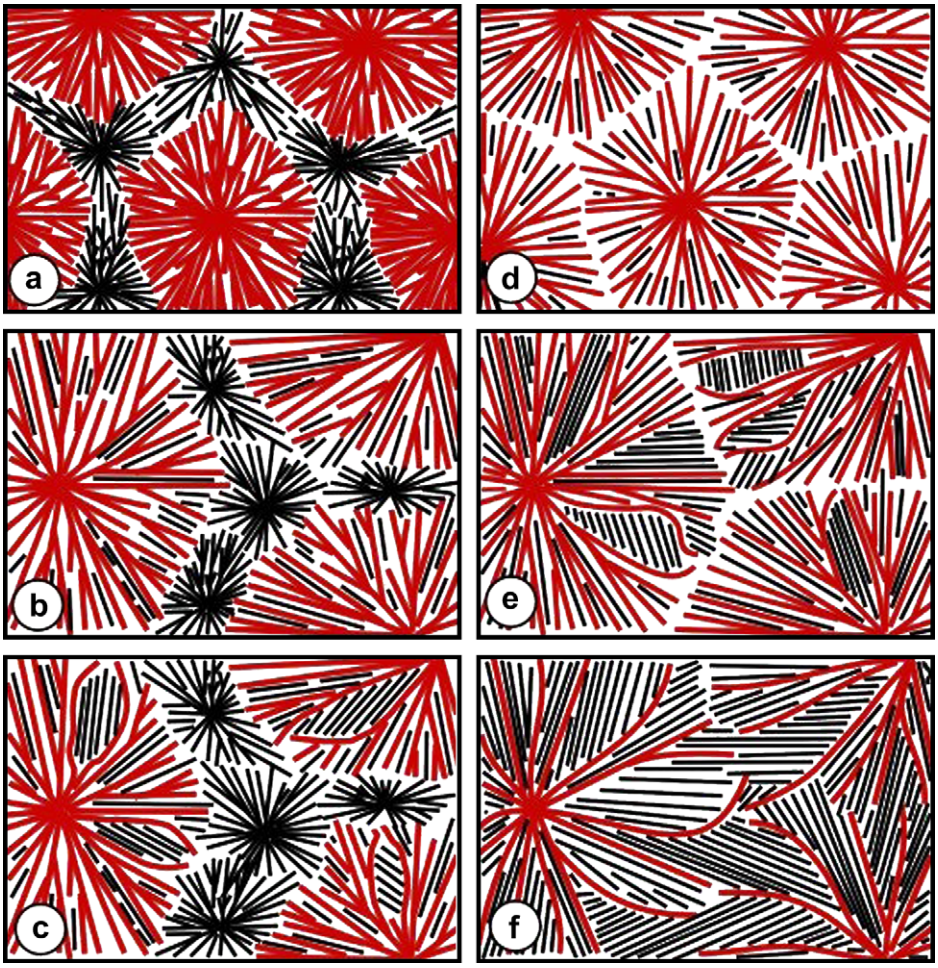

Fig. 15. Sketches describing the phase segregation processes of different PBS/PBA blends at different temperatures. The red lines represent PBS, while the black ones represent the PBA crystals. Parts a, b and c correspond to the crystallization of PBS at 100 °C followed by quenching to low temperature for PBA crystallization, whereas parts d, e and f are related to PBS crystallized at 75 °C.

structures are really not related to phase separation taken place before crystallization, another experiment was performed. In a remarkable recent series of papers, Wang and coworkers [21–23] have allowed polymer blends to undergo partial liquid/liquid phase separation at a temperature below the UCST, and then quenched to crystallize the blend isothermally at a lower temperature. The result is always to produce morphologies significantly different from those produced by directly quenching from above the UCST to the same crystallization temperature. We have performed a similar experiment on the PBS/PBA system. As shown in Fig. 16, a PBS/PBA 80/20 blend was quenched from the melt to 100 °C and held there for 15 h and then quenched again from this temperature to 75 °C for isothermal crystallization. After 15 h at 100 °C, only one PBS spherulite appears in the view field in the center part of the picture as indicated by a white arrow. The remaining melt then crystallizes at 75 °C exactly as does an 80/20 blend quenched directly to 75 °C. The absence of an effect of the thermal treatment at the higher temperature on crystallization at the lower temperature demonstrates that there has been no liquid/liquid phase separation at 100 °C.

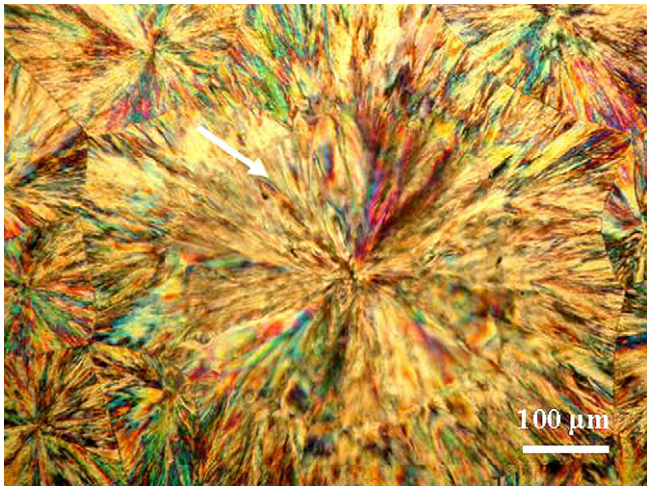

Fig. 16. An optical micrograph of a PBS/PBA 80/20 blend quenched from the melt to 100 °C for 15 h and then quenched again from this temperature to 75 °C for isothermal crystallization. The arrow indicates the spherulite formed at 100 °C.

The above discussion unambiguously indicates that the observed structures are caused by crystallization induced phase separation. Therefore, we discuss here the morphological development in this blend system as resulting from kinetic and mass balance inputs. In the present case, both the PBS and the PBA components are capable of crystallization over a wide range of composition. Since the two components cannot co-crystallize and the crystallization of each component occurs in well-separated temperature regions, the rejection of PBA by the crystallizing PBS affects the kinetics and morphology of PBS, and thereby controls also the space

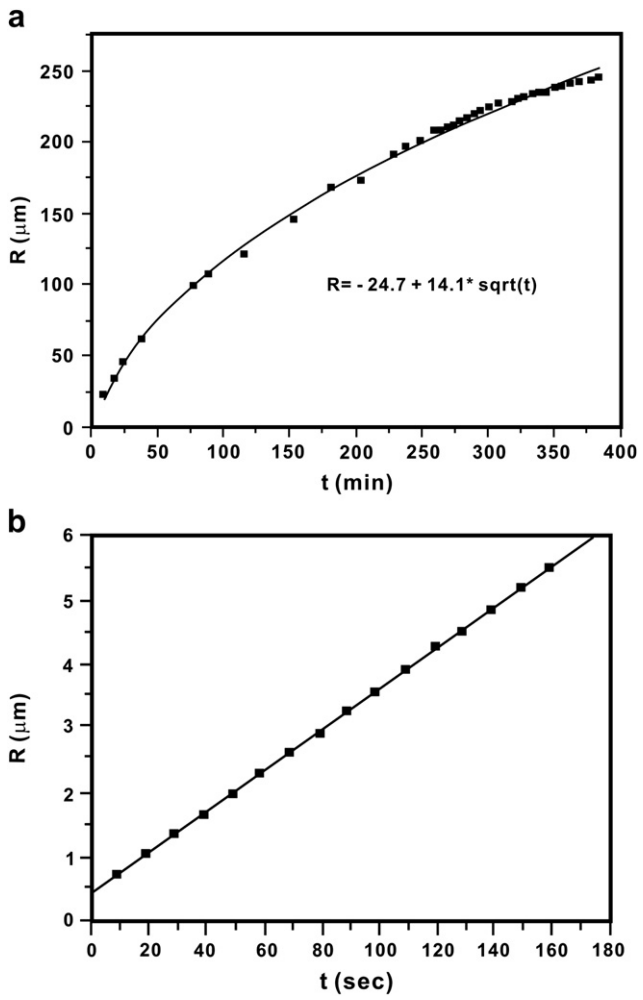

Fig. 17. Radius of PBS spherulites versus crystallization time for PBS/PBA 80/20 blend crystallizing at (a) 100 °C and (b) 75 °C. The line in (a) is the least squares parabolic fit and the line in (b) is the least squares linear fit.

available for subsequent crystallization of PBA. The phase separation in crystalline blends during the crystallization of one component can be understood in terms of the diffusion length $\delta = D/G$, where D is the diffusion coefficient of the noncrystallizable species in the blend and G is the radial growth rate of the spherulites. The diffusion length is a quantitative measure of the distance a noncrystallizable chain can move in the melt ahead of the crystallization front. If the diffusion length δ is sufficiently small, the noncrystallizable component can diffuse no farther than into the interlamellar region of the crystallizing component. For an intermediate range of δ, the noncrystallizable component should locate between the fibrils (also known as growth arms), and at large δ, between spherulites [1,17,24,25].

The above results can be qualitatively explained on the basis of the diffusion length δ. To estimate the δ, the crystal growth rate G of PBS at varying crystallization temperatures was measured. It is found that the crystal growth rate of PBS in different blends at 75 °C is ca. 2 orders of magnitude higher than that grown at 100 °C. At the same time, the diffusivity D of PBA melt in front of growing PBS crystals should decrease with decreasing temperature. Therefore, diffusion length can be increased by more than a factor of 100 as the crystallization temperature is increased. This leads to PBA in an 80/20 blend being excluded from the growing PBS spherulites at 100 °C, as sketched in Fig. 15a, while at 75 °C all PBA retain within the growing spherulite and crystallize between PBS lamellae or fibrils (growth arms), as sketched in Fig. 15d. If this is true, the PBA component will build up more and more ahead of the growing PBS spherulite and slow down its growth at 100 °C. This situation should manifest a $R \propto t^{1/2}$ relationship between the spherulite radius and time [24–26]. On the other hand, the inclusion of PBA within the PBS spherulites at 75 °C indicates that the PBS fibrils (or growth arms) exclude PBA at their growing tips. As a consequence, a steady state ($R \propto t$) should be established. That these scenarios are correct can be seen from the growth kinetics curves shown in Fig. 17. There we see that at 100 °C the PBS spherulite radius increases with the inverse square root of time, whereas the radius increases linearly with time at 75 °C.

When the PBA content is increased to 50%, the diluting effect of PBA on PBS becomes evident. This leads to PBS crystallizing in a relatively more open structure, which makes it necessary to retain a substantial portion of molten PBA melt in the interlamellar and interfibrillar regions of PBS, even at high temperature (100 °C). Therefore, besides the portion of PBA expelled to the interspherulitic region of PBS, some of PBA must crystallize between the PBS lamellae, leading to the concurrence of interspherulitic and interlamellar phase segregations as sketched in Fig. 15b. During the lower temperature (75 °C) crystallization of this blend, the smaller diffusion length acts to confine all of PBA within the PBS spherulites. At the same time, the large concentration of PBA within the PBS spherulites requires that the PBS spherulite be more open, or skeletal. As a consequence, domains of mainly PBA will form between the intraspherulitic fibrils. In Fig. 15e this is sketched as parallel-aligned PBA lamellar regions within the PBS spherulites. With further increase of the PBA component to 80%, at high temperature, a mass balance demands that PBS forms very sparse, skeletal spherulites. This results in the concurrence of interlamellar, interfibrillar and interspherulitic crystallization of PBA, as depicted in Fig. 15c. At lower temperature, 75 °C in present study, due to the much fast crystallization process of PBS with poor chain mobility of PBA, PBS forms only a spherulitic scaffold. PBA fills in the PBS scaffold and adopts interfibrillar crystallization, as depicted in Fig. 15f.

5. Conclusions

We have investigated the morphological features of the PBS/PBA blends varying in blend ratio at different crystallization temperatures of the high melting PBS component. It was found that the PBA melt segregates in different manners depending on crystallization temperature of PBS. Interspherulitic phase segregation of PBA takes place at high temperature, e.g. 100 °C, for all blend compositions due to the high diffusion length. On the other hand, no interspherulitic phase separation of PBA takes place at 75 °C for all blend compositions, since the diffusion length is too small to permit diffusion over such large distances. It was further found that the PBA melt acting as a diluent affects the morphology of PBS, which in turn affects phase separation behavior of PBA remarkably. At 100 °C, in blends with PBA as a minority phase, only interspherulitic phase segregation of PBA takes place. With increasing PBA concentration, the resultant open structure of PBS caused by diluting effect of PBA melt makes it necessary to retain some portion of the PBA melt in between the PBS lamellae, which leads to the concurrence of interlamellar and interspherulitic phase segregations. An even higher PBA content leads to the occurrences of all three phase separation options, i.e. interlamellar, interfibrillar and interspherulitic phase segregations. At 75 °C, in blend with PBA as a minority phase, mainly interlamellar segregation of PBA occurs. For a 50/50 blend, interlamellar and interfibrillar phase segregations take place simultaneously. For a PBA in-rich blend, PBS forms only a spherulitic framework filled in with the PBA lamellar

crystals, indicating that interfibrillar mode is the main phase separation process.

Acknowledgements

The financial support of the Outstanding Youth Fund and the National Natural Science Foundations of China (No. 50521302, 20423003, 20574079, 20634050 and 20604031) are gratefully acknowledged.

References

[1] Keith HD, Padden FJ. J Appl Phys 1964;35:1270.
[2] Russell TP, Ito H, Wignall GD. Macromolecules 1988;21:1703.
[3] Runt JP, Zhang X, Miley DM, Gallagher KP, Zhang A. Macromolecules 1992;25:3902.
[4] Defieuw G, Groeninckx G, Reynaers H. Polymer 1989;30:595.
[5] Crevecoeur G, Groeninckx G. Macromolecules 1991;24:1190.
[6] Dong LS, Olley RH, Bassett DC. J Mater Sci 1998;33:4043.
[7] Shabanaa HM, Olleya RH, Bassetta DC, Jungnickel BJ. Polymer 2000;41:5513.
[8] Cheung YW, Stein RS, Wignall GD, Yang HE. Macromolecules 1993;26:5365.
[9] Penning JP, Manley RStJ. Macromolecules 1996;29:77.
[10] Liu LZ, Chu B, Penning JP, Manley RStJ. Macromolecules 1997;30:4398.
[11] Okerberg BC, Marand H, Douglas JF. Polymer 2008;49:579.
[12] Castro FA, Carlos FO Graeff, Heier J, Hany R. Polymer 2007;48:2380.
[13] Qiu Z, Ikehara Nishi T. Polymer 2003;44:3095.
[14] Wang HJ, Schultz JM, Yan SK. Polymer 2007;48:3530.
[15] Hou WM, Zhou JJ, Gan ZH, Shi AC, Chan CM, Li L. Polymer 2007;48:4926.
[16] Qiu Z, Yan C, Lu J, Yang W, Ikehara T, Nishi T. J Phys Chem B 2007;111:2783.
[17] Hudson SD, Davis DD, Lovinger AJ. Macromolecules 1992;25:1759.
[18] Jonas AM, Ivanov DA. Macromolecules 1998;31:4546.
[19] Ikehara T, Nishikawa Y, Nishi T. Polymer 2003;44:6657.
[20] Kanamoto T. J Polym Sci Polym Phys Ed 1974;12:2535.
[21] Wang H, Shimizu K, Kim H, Hobbie EK, Wang ZG, Han CC. J Chem Phys 2002;116:7311.
[22] Matsuba G, Shimizu K, Wang H, Wang Z, Han CC. Polymer 2004;45:5137.
[23] Zhang X, Wang Z, Dong X, Wang D, Han CC. J Chem Phys 2006;125:24907.
[24] Tanaka H, Nishi T. Phys Rev A 1989;39:783.
[25] Schultz JM. Polymer 1991;32:3268.
[26] Schultz JM. Polymer crystallization. Oxford, UK: Oxford University Press; 2001 [chapter 10].